Research Square

Preprints are preliminary reports that have not undergone peer review.
They should not be considered conclusive, used to inform clinical practice,
or referenced by the media as validated information.

Three-dimensional morphometry of the normal nasal septum on computed tomography: sex- and age-specific reference values from 1,373 adults

Michael Sramek

sramek.michael@mayo.edu

Mayo Clinic in Arizona

Hannah Gibbs

Mayo Clinic in Arizona

Amar Miglani

Mayo Clinic in Arizona

Tanya Rath

Mayo Clinic in Arizona

Stephen Bansberg

Mayo Clinic in Arizona

Michael Marino

Mayo Clinic in Arizona

Research Article

Keywords: nasal septum, morphometry, reference values, computed tomography, deep learning, septoplasty

Posted Date: November 1st, 2026

DOI: https://doi.org/10.21203/rs.3.rs-11297009/v1

License: This work is licensed under a Creative Commons Attribution 4.0 International License.
Read Full License

Additional Declarations: No competing interests reported.

Abstract

Purpose.

Normative data for the three-dimensional anatomy of the nasal septum are sparse. We applied automated segmentation to a large series of adults with radiologically normal sinonasal anatomy to establish sex- and age-specific reference values for septal size, thickness, and midline deviation.

Methods.

Retrospective cross-sectional study of 1,373 adults (394 men, 979 women; age 18 to 90 years) with sinus computed tomography reported as normal. The septum was segmented by a validated three-dimensional convolutional network (held-out Dice 0.983), and 12 parameters were computed from each segmentation: volume, surface area, maximal and mean sagittal cross-sectional area, three linear extents, three thickness measures, and maximal midline deviation and deviation angle. Reference percentiles were computed by sex and by sex within four age bands; age trends were estimated by linear and quantile regression.

Results.

Median septal volume was 16,710 mm^3 in men (5th to 95th percentile 13,594 to 20,455) and 12,500 mm^3 in women (9,963 to 15,329); median mean thickness was 4.89 and 4.29 mm. All size and thickness parameters were larger in men. In men, volume, depth, height, and maximal thickness increased by 1.2 to 1.4% per decade of age; in women they were constant (sex-by-age interaction $P \leq 0.021$). Midline deviation did not vary with age, and its 95th percentile was about 3 mm in both sexes.

Conclusion.

These sex- and age-specific percentiles provide a quantitative reference for interpreting septal anatomy on computed tomography, planning septal surgery, and selecting reference geometries for airflow modeling.

Introduction

The nasal septum is the central partition of the nasal cavity and the principal determinant of its sagittal geometry. It is also the structure most often operated on in rhinologic practice, yet quantitative anatomical reference data for it are thin. Earlier morphometric work measured the septum in two dimensions on single axial or coronal slices, in cadaveric specimens, or in computed tomography (CT) series of fewer than 200 individuals [6, 14, 25]. The largest three-dimensional study to date reconstructed the septum manually in 96 adults [25]. Two-dimensional measurements depend on the slice chosen and

on head position at acquisition, and small series cannot characterize the tails of the distribution, which are the clinically relevant region when a surgeon asks whether a given septum is unusually thick, long, or deviated.

A reference standard for septal anatomy has practical uses beyond description. For septoplasty and septorhinoplasty, knowing where an individual falls relative to a sex- and age-matched population informs expectations about available cartilage and bone and about the degree of correction required [9, 15]. For computational fluid dynamics (CFD) modeling of nasal airflow, the geometry of the airway is sensitive to segmentation choices, and standard reference anatomies against which an individual model can be compared have not been established [4, 12, 16]. For radiologic reporting, septal deviation is so common in unselected adults [1, 15, 23] that a quantitative threshold for "normal" is needed before deviation on imaging can be interpreted.

Deep-learning segmentation now makes it possible to measure complex anatomy reproducibly at scale. Convolutional networks of the nnU-Net family [10] segment paranasal sinus structures with Dice coefficients above 0.9 [5, 19, 24], and benchmark datasets for sinonasal segmentation have been released [27]. Applications to the septum specifically have concentrated on classifying deviation [11, 26] rather than on measuring the structure. We previously developed and validated a three-dimensional network that segments the entire osteocartilaginous septum from clinical sinus CT and used it to show that septal sexual dimorphism is almost entirely a matter of size rather than shape [20]. Here we use the same segmentations to address a different and more practical question: what are the normal ranges of septal size, thickness, and midline deviation in adults, how do they differ between the sexes, and how do they change with age? The product is a set of sex- and age-specific reference percentiles for 12 segmentation-derived parameters, intended for clinical interpretation of individual scans and as reference geometry for airway modeling.

Materials and methods

Study design and population

This retrospective cross-sectional study was conducted at a single tertiary academic medical center under institutional review board approval (Mayo Clinic IRB 25-008837) with a waiver of informed consent for the use of de-identified imaging and record data. The study conforms to the Declaration of Helsinki, and reporting follows the STROBE recommendations for cross-sectional studies [22].

Adults who underwent non-contrast sinus CT between 2018 and 2025 with a radiology impression of "normal" or equivalent were identified. Examinations with documented prior nasal or sinus surgery, cleft palate, or septal perforation on the index study were excluded after line-by-line review of the radiology impression. All examinations were acquired under routine clinical protocols on multidetector scanners from several manufacturers, with axial slice thickness of 1.0 mm or less and a bone-kernel reconstruction. Of 1,673 segmented septa, 1,567 belonged to individuals with sex recorded in the

institutional record. One examination per individual was retained (23 repeat examinations removed), individuals with a septoplasty or septal repair recorded before the index scan were excluded (n = 27), one segmentation that failed automated quality control was removed, individuals younger than 18 years at the scan were excluded (n = 31), and 112 individuals whose scan date could not be retrieved (so that adult status and age could not be confirmed) were excluded. The analytic cohort therefore comprised 1,373 adults, identical to the cohort of the companion study of sexual dimorphism [20].

Sex was taken as the sex recorded in the electronic health record. Age at scan was computed from date of birth and scan date, and four age bands were defined a priori: 18 to 39, 40 to 59, 60 to 79, and 80 years and older. Race and ethnicity are reported as the self-identified categories in the health record to describe the composition of the cohort.

Segmentation

Digital Imaging and Communications in Medicine series were converted to Neuroimaging Informatics Technology Initiative format [13]. Septa were segmented with a three-dimensional residual-encoder nnU-Net, version 2 [10], in the full-resolution configuration with default preprocessing. The model was trained on 125 examinations manually segmented by an otolaryngology resident in 3D Slicer [8] under iterative review by a fellowship-trained rhinologist, with five-fold cross-validation (mean Dice 0.957). The segmentation protocol captured the entire osteocartilaginous septum from the nasal floor to the skull base and from the membranous septum to the sphenoid rostrum, including the quadrangular cartilage, vomer, and perpendicular plate of the ethmoid. On 24 held-out examinations the five-fold ensemble achieved a Dice similarity coefficient of 0.983 (SD 0.005; range 0.974 to 0.991), a 95th-percentile Hausdorff distance of 1.82 mm (SD 0.43), and an average symmetric surface distance of 0.31 mm (SD 0.08) [21]. Training used the framework's default configuration (stochastic gradient descent with Nesterov momentum, initial learning rate 0.01 with polynomial decay, combined Dice and cross-entropy loss, deep supervision, standard augmentation, 1,000 epochs per fold) on a workstation with a 16 GB NVIDIA graphics card; inference used the ensemble with test-time mirroring. Output masks were screened by automated rules for volume, extent, and connectivity, and flagged masks were reviewed manually.

Morphometric parameters

Twelve parameters were computed deterministically from each binary mask in Python using SimpleITK, scikit-image, trimesh, and NumPy, in the scanner-defined right-anterior-superior frame (Fig. 1). Septal volume (mm^3) is the sum of voxel volumes. Surface area (mm^2) is the summed face area of a marching-cubes mesh. Maximal and mean sagittal cross-sectional area (CSA, mm^2) are the maximum and mean in-plane septal area across sagittal slices sampled through the mask at the native in-plane resolution; the slice of maximal CSA is shown in Fig. 1b. Anterior-posterior depth, medial-lateral width, and cranial-caudal height (mm) are the extents of the mask along the three axes. Local septal thickness was

computed on the mesh as twice the distance from each surface vertex to the medial skeleton of the septum (Fig. 1c) and summarized as its mean, 95th percentile, and maximum (mm). Midline deviation was quantified on coronal slices: the medial-lateral centroid of the septum was computed at each cranial-caudal level, a straight line was fitted to these centroids by least squares, the maximal perpendicular distance of a centroid from that line was recorded as the maximal midline deviation (mm), and the angle between the fitted line and the cranial-caudal axis was recorded as the deviation angle (degrees; Fig. 1d). The fitted line is derived from the segmentation alone and uses no external skull landmarks, so the deviation measures describe the septum's departure from its own best-fit plane rather than from the facial midline. Thickness could not be computed for one manually segmented examination, so thickness parameters are reported for 1,372 individuals.

Statistical analysis

For each parameter and sex, the mean, standard deviation, and the 5th, 25th, 50th, 75th, and 95th percentiles were computed empirically, with a 95% confidence interval for the median from 2,000 bootstrap resamples. The same percentiles were computed within each sex-by-age-band stratum. Age trends were estimated by ordinary least-squares regression of each parameter on age within each sex, expressed as the change per decade with its 95% confidence interval and as a percentage of the sex-specific mean, together with the Spearman rank correlation; a sex-by-age interaction was tested in a model with both sexes. To display how the whole reference distribution shifts with age, linear quantile regression was fitted at the 5th, 25th, 50th, 75th, and 95th percentiles for four representative parameters. Between-sex differences are summarized briefly as the percentage difference and Cohen's d; their detailed analysis, including allometric adjustment, is the subject of the companion report [20]. Analyses used Python 3.10 with NumPy, pandas, SciPy, and statsmodels; two-sided alpha was 0.05.

Use of artificial intelligence tools

A large language model (Claude, Anthropic) was used, under the direction and review of the authors, to assist with writing and reviewing the analysis scripts, with drafting and editing the manuscript text, and with checking reported values against the analysis output. The authors designed the study, chose the variables and analyses, interpreted the results, verified the code and every reported value, and take full responsibility for the content. No identifiable patient data were provided to the tool.

Results

Cohort

The cohort comprised 1,373 adults, 394 men (28.7%) and 979 women, with a mean age of 54.5 years (SD 16.5; range 18 to 90) that did not differ by sex (Table 1). The age bands contained 291, 491, 535, and 56 individuals, with at least 19 men and 37 women in every band. By health-record categories, 90.8% of

individuals were recorded as White and 6.8% as Hispanic or Latino; the median Charlson comorbidity index was 1.

Table 1
Characteristics of the cohort

Characteristic	Men	Women	All
n	394	979	1,373
Age at scan, years, mean (SD)	54.4 (17.1)	54.5 (16.2)	54.5 (16.5)
Age range, years	18 to 90	18 to 90	18 to 90
Age 18 to 39 years, n (%)	91 (23.1)	200 (20.4)	291 (21.2)
Age 40 to 59 years, n (%)	137 (34.8)	354 (36.2)	491 (35.8)
Age 60 to 79 years, n (%)	147 (37.3)	388 (39.6)	535 (39.0)
Age 80 and older years, n (%)	19 (4.8)	37 (3.8)	56 (4.1)
Recorded as White, n (%)	349 (88.6)	897 (91.6)	1,246 (90.8)
Recorded as Hispanic or Latino, n (%)	26 (6.6)	68 (6.9)	94 (6.8)
Charlson comorbidity index, median (IQR)	1 (0 to 3)	1 (0 to 2)	1 (0 to 2)

Race and ethnicity are the self-identified categories recorded in the electronic health record. SD standard deviation, IQR interquartile range

Reference values by sex

Table 2 gives the mean, standard deviation, and reference percentiles of the 12 parameters by sex. Median septal volume was 16,710 mm^3 in men (5th to 95th percentile 13,594 to 20,455) and 12,500 mm^3 in women (9,963 to 15,329); the female 95th percentile lay below the male median. Median anterior-posterior depth was 92.8 mm in men (83.9 to 100.4) and 84.7 mm in women (77.0 to 90.9); median cranial-caudal height was 53.8 and 49.6 mm; median medial-lateral width was 16.2 and 14.6 mm. Mean septal thickness had a median of 4.89 mm in men (4.08 to 5.71) and 4.29 mm in women (3.54 to 5.09); the 95th percentile of local thickness, which captures the thick vomerine and maxillary-crest regions, had a median of 9.84 mm in men and 8.89 mm in women, and maximal thickness 14.0 and 12.7 mm.

Table 2
Reference values for 12 septal morphometric parameters by sex: mean, standard deviation, and percentiles

Parameter	Sex	n	Mean (SD)	P5	P25	P50	P75	P95	95% CI of median
Septal volume (mm^3)	Men	394	16,852 (2,183)	13,594	15,372	16,710	18,298	20,455	16,538 to 17,015
	Women	979	12,564 (1,686)	9,963	11,362	12,500	13,661	15,329	12,365 to 12,623
Surface area (mm^2)	Men	394	8,781 (682)	7,665	8,343	8,781	9,220	9,814	8,709 to 8,880
	Women	979	7,409 (603)	6,469	7,028	7,405	7,790	8,480	7,344 to 7,443
Maximum sagittal CSA (mm^2)	Men	394	2,661 (477)	1,836	2,336	2,696	3,019	3,391	2,656 to 2,755
	Women	979	2,231 (413)	1,510	1,972	2,259	2,515	2,832	2,223 to 2,304
Mean sagittal CSA (mm^2)	Men	394	1,015 (155)	773	907	1,008	1,119	1,292	987 to 1,028
	Women	979	836 (129)	630	749	831	924	1,057	821 to 842
Anterior-posterior depth (mm)	Men	394	92.7 (4.9)	83.9	89.4	92.8	95.5	100.4	92.4 to 93.5
	Women	979	84.3 (4.7)	77.0	81.6	84.7	87.3	90.9	84.3 to 85.0
Medial-lateral width (mm)	Men	394	16.5 (2.3)	13.2	15.0	16.2	17.8	20.4	16.0 to 16.5
	Women	979	14.9 (2.1)	11.9	13.4	14.6	16.2	18.6	14.4 to 14.7
Cranial-caudal	Men	394	54.2 (4.6)	47.5	51.0	53.8	57.0	62.7	53.4 to 54.4

Parameter	Sex	n	Mean (SD)	P5	P25	P50	P75	P95	95% CI of median
height (mm)									
	Women	979	49.9 (4.0)	44.0	47.2	49.6	52.2	57.6	49.2 to 49.8
Mean thickness (mm)	Men	393	4.89 (0.52)	4.08	4.56	4.89	5.19	5.71	4.85 to 4.93
	Women	979	4.30 (0.46)	3.54	3.99	4.29	4.58	5.09	4.25 to 4.33
95th-percentile thickness (mm)	Men	393	9.89 (1.09)	8.30	9.14	9.84	10.55	11.76	9.67 to 9.90
	Women	979	8.94 (1.03)	7.29	8.30	8.89	9.65	10.66	8.79 to 9.01
Maximum thickness (mm)	Men	393	14.0 (1.5)	11.4	13.0	14.0	15.1	16.8	13.7 to 14.2
	Women	979	12.8 (1.3)	10.7	11.9	12.7	13.7	15.0	12.7 to 12.9
Maximum midline deviation (mm)	Men	394	1.55 (0.85)	0.63	0.96	1.31	1.89	3.27	1.24 to 1.40
	Women	979	1.34 (0.78)	0.49	0.83	1.13	1.65	2.88	1.08 to 1.18
Deviation angle (°)	Men	394	0.63 (3.03)	-4.43	-1.21	0.49	2.41	5.52	0.14 to 0.83
	Women	979	0.43 (3.00)	-4.47	-1.54	0.38	2.34	5.45	0.16 to 0.72

P5 to P95, empirical 5th to 95th percentiles. The confidence interval of the median is from 2,000 bootstrap resamples. Thickness parameters are available for 393 men. CSA sagittal cross-sectional area, SD standard deviation, CI confidence interval

All size and thickness parameters were larger in men, by 34% for volume (Cohen's d = 2.33), 19% for surface area (d = 2.19), 10% for depth (d = 1.79), 14% for mean thickness (d = 1.23), and 9 to 21% for the remaining size parameters (d 0.74 to 1.31). Midline deviation differed only slightly by sex: the median maximal deviation was 1.31 mm in men and 1.13 mm in women (d = 0.26), and its 95th percentile was

3.27 and 2.88 mm. The deviation angle was centered near zero in both sexes (median 0.49° and 0.38°) with a 5th to 95th percentile span of about 10° (Table 2), and did not differ by sex (P = 0.29).

Reference values by sex and age band

Percentiles within each sex-by-age-band stratum are provided in Online Resource 1 (Table S1). In men, the median volume rose from 16,235 mm³ at 18 to 39 years to 17,141 mm³ at 60 to 79 years, and the median anterior-posterior depth from 91.4 to 93.9 mm; the 95th percentile of volume rose from 19,461 to 21,307 mm³. In women, the median volume was 12,397, 12,476, 12,527, and 12,944 mm³ across the four bands, and median depth 84.0, 84.8, 84.9, and 83.5 mm. Median mean thickness was stable across bands in both sexes (4.88 to 4.93 mm in men, 4.25 to 4.40 mm in women).

Age trends

Table 3 gives the linear change per decade of age for each parameter by sex. In men, septal volume increased by 231 mm³ per decade (95% CI 106 to 355; 1.4% of the male mean), surface area by 83 mm² (0.9%), anterior-posterior depth by 0.53 mm (0.6%), cranial-caudal height by 0.62 mm (1.2%), medial-lateral width by 0.18 mm (1.1%), and maximal thickness by 0.18 mm (1.3%), each P < 0.01. In women, volume (44 mm³ per decade; 0.3%; P = 0.19), depth (0.10 mm; P = 0.26), and mean thickness did not change, while surface area (0.4% per decade), cranial-caudal height (0.5%), medial-lateral width (1.0%), and maximal thickness (0.9%) increased slightly. The sex-by-age interaction was significant for volume (P = 0.004), surface area (P = 0.021), depth (P = 0.011), and height (P = 0.009), indicating that the male and female septa diverge further with age. Mean and 95th-percentile thickness, maximal and mean CSA, maximal midline deviation, and the deviation angle showed no material age trend in either sex (all |rho| ≤ 0.14).

Table 3
Change in each parameter per decade of age, by sex

Parameter	Men: change per decade (95% CI)	Men: % of mean	Men: P	Women: change per decade (95% CI)	Women: % of mean	Women: P	Sex-by-age interaction P
Septal volume (mm^3)	230.8 (106.2 to 355.4)	+ 1.4	< 0.001	43.6 (-21.6 to 108.8)	+ 0.3	0.189	0.004
Surface area (mm^2)	83.3 (44.5 to 122.0)	+ 0.9	< 0.001	32.2 (8.9 to 55.4)	+ 0.4	0.007	0.021
Maximum sagittal CSA (mm^2)	3.3 (-24.4 to 31.0)	+ 0.1	0.815	-8.2 (-24.2 to 7.7)	-0.4	0.312	0.452
Mean sagittal CSA (mm^2)	3.8 (-5.2 to 12.7)	+ 0.4	0.411	-5.2 (-10.2 to -0.2)	-0.6	0.041	0.066
Anterior-posterior depth (mm)	0.53 (0.25 to 0.81)	+ 0.6	< 0.001	0.10 (-0.08 to 0.28)	+ 0.1	0.257	0.011
Medial-lateral width (mm)	0.18 (0.05 to 0.31)	+ 1.1	0.006	0.15 (0.07 to 0.23)	+ 1.0	< 0.001	0.691
Cranial-caudal height (mm)	0.62 (0.37 to 0.88)	+ 1.2	< 0.001	0.24 (0.08 to 0.39)	+ 0.5	0.002	0.009
Mean thickness (mm)	0.023 (-0.007 to 0.053)	+ 0.5	0.139	-0.002 (-0.020 to 0.016)	-0.1	0.798	0.143
95th-percentile thickness (mm)	0.084 (0.021 to 0.147)	+ 0.9	0.009	0.017 (-0.022 to 0.057)	+ 0.2	0.394	0.071
Maximum thickness (mm)	0.18 (0.09 to 0.27)	+ 1.3	< 0.001	0.11 (0.06 to 0.16)	+ 0.9	< 0.001	0.149
Maximum midline deviation (mm)	0.027 (-0.022 to 0.076)	+ 1.7	0.287	0.021 (-0.009 to 0.052)	+ 1.6	0.163	0.857
Deviation angle (°)	0.084 (-0.092 to 0.259)	+ 13.4	0.350	0.030 (-0.086 to 0.146)	+ 6.9	0.612	0.616

Change per decade is the slope of an ordinary least-squares regression of the parameter on age within each sex, with its 95% confidence interval, and as a percentage of the sex-specific mean. The interaction P-value tests whether the slope differs between sexes. CSA sagittal cross-sectional area, CI confidence interval

Quantile regression (Fig. 2) shows that in men the whole volume distribution shifts upward with age, more at the upper percentiles (95th percentile + 449 mm³ per decade) than at the lower (5th percentile + 125 mm³ per decade), so that the normal range widens with age. The female distributions of volume, depth, and thickness are flat across adult life. Maximal midline deviation is flat at the median in both sexes, with a modest widening of the 95th percentile in men (3.07 mm at age 30 to 3.42 mm at age 70).

Discussion

This study provides sex- and age-specific reference percentiles for 12 three-dimensional parameters of the nasal septum, derived from 1,373 adults with radiologically normal sinonasal anatomy by a validated automated segmentation. To our knowledge it is the largest quantitative description of septal anatomy to date, by more than an order of magnitude over the largest previous three-dimensional series [25], and the first to report thickness and midline deviation percentiles by sex and age. Three findings have direct anatomical and clinical relevance.

First, the normal range is wide and strongly sex-dependent. The 5th to 95th percentile of volume spans about 7,000 mm³ within each sex, and the female 95th percentile lies below the male median. Sex differences in nasal airway dimensions have been reported before at smaller scale [3, 18]; here they are large enough that pooled reference values would misclassify a substantial fraction of individuals; a volume of 15,000 mm³ is near the 75th percentile for a woman and near the 20th for a man. The same applies to depth, height, and thickness. The companion analysis showed that these sex differences are almost entirely a matter of size, with little residual shape difference after allometric adjustment [20], which is why we present the reference values stratified by sex rather than normalized to a shape space.

Second, the septum continues to enlarge slowly through adult life in men but not in women. Male volume, depth, height, and maximal thickness increase by roughly 1.2 to 1.4% per decade, and the upper percentiles of volume increase faster than the lower, so the male normal range widens with age; the corresponding female distributions are flat, and the sex-by-age interaction is significant for the principal size parameters. Continued adult growth of the facial skeleton, including the nasal region, has been described in longitudinal and cross-sectional studies [2, 7, 17], and cross-sectional CT work has reported that intranasal air volume increases with age [14]. Our data place the septum among the structures that change, and localize the change to men. A cross-sectional design cannot separate within-individual growth from secular trends in body size between birth cohorts, and the latter would be expected to act in the opposite direction (younger cohorts larger), so the observed increase is unlikely to be a cohort artifact; a longitudinal series would settle the question. Clinically, the result means that an older man's

septum should be judged against the reference values for his age band rather than against those of young adults.

Third, midline deviation is common, moderate in degree, and independent of age and nearly of sex. The median maximal deviation from the septum's own best-fit plane was 1.1 to 1.3 mm and the 95th percentile about 3 mm in individuals whose CT was reported as normal. Earlier population studies found deviation in 20 to 80% of unselected adults depending on definition [1, 15, 23]; our continuous measure provides a threshold for that definition: a maximal deviation above about 3 mm from the best-fit plane lies outside the 95th percentile of adults with a normal radiology report. The deviation angle was centered on zero with a spread of about ± 5°, which quantifies the normal obliquity of the septum relative to the cranial-caudal axis. Because our deviation measures are referenced to the septum's own best-fit plane rather than to the facial midline, they describe septal curvature and buckling rather than displacement of the whole septum, and the two should not be confused when comparing with clinical grading systems.

Clinical and modeling applications

The reference tables are intended to be used at the level of the individual scan. An automated segmentation of a patient's septum yields the same 12 parameters within seconds, and each can be placed on the sex- and age-specific percentile scale in Table 2 and Online Resource 1. For surgical planning, the thickness percentiles indicate how much bone and cartilage is likely to be available for harvest or resection, and the depth and height percentiles frame the dimensions of the field; an unusually thick posterior septum, for example, bears on the choice of instrument and the expected difficulty of vomerine resection. For CFD modeling, in which results are sensitive to the geometry supplied [4, 16], a median male and a median female septum defined by these percentiles provide reproducible reference geometries, and an individual model can be reported with its percentile position. For radiologic reporting, the deviation percentiles give the first quantitative definition of normal septal curvature on CT.

Limitations

The cohort is from a single institution and is predominantly recorded as White, so the reference values should be applied to other populations only after local validation, particularly for the size parameters, which track body and facial size. Individuals were imaged for sinonasal symptoms and the cohort is not a probability sample of the population, although the restriction to examinations reported as normal removes inflammatory disease and prior surgery. Body height and weight were not available, so the size parameters could not be indexed to stature. The deviation measures use a segmentation-derived best-fit plane rather than the facial midline, which maximizes reproducibility but differs from clinical grading conventions. The age analysis is cross-sectional. Finally, the segmentation applies to CT; the cartilaginous septum is not visible on dry bone, and the thickness and volume values include cartilage, mucoperichondrium is excluded by the bone-kernel protocol, and the values are therefore not directly comparable with cadaveric measurements of bone alone.

Conclusion

Automated three-dimensional segmentation of clinical sinus CT yields reproducible, sex- and age-specific reference values for septal volume, surface area, cross-sectional area, linear dimensions, thickness, and midline deviation in adults. Men have larger septa than women in every size parameter, the male septum continues to enlarge slowly with age while the female septum does not, and midline deviation of up to about 3 mm from the septum's own best-fit plane is within the normal range. The percentile tables provide a quantitative standard for interpreting individual scans, planning septal surgery, and selecting reference geometries for airflow modeling.

Declarations

Funding: No funding was received for this study.

Competing interests: The authors have no relevant financial or non-financial interests to disclose.

Ethics approval: The study was approved by the Mayo Clinic Institutional Review Board (protocol 25-008837) and was performed in accordance with the Declaration of Helsinki.

Consent to participate: The Institutional Review Board granted a waiver of informed consent for this retrospective analysis of de-identified imaging and record data.

Consent to publish: Not applicable; the figures contain no identifiable patient information.

Data availability: The computed tomography examinations cannot be shared because they are identifiable medical images held under institutional policy. The de-identified per-individual dataset (recorded sex, age at scan, and the 12 parameters) and the analysis code are held by the corresponding author and can be made available to qualified researchers on reasonable request, subject to Mayo Clinic institutional review and a data use agreement. All reference percentiles are reported in full in Table 2 and Online Resource 1.

Author contributions: Michael Sramek: conceptualization, methodology, software, formal analysis, investigation, data curation, visualization, writing (original draft and revision). Hannah Gibbs: investigation, data curation, writing (review and editing). Amar Miglani: investigation, methodology, validation, writing (review and editing). Tanya Rath: data curation, validation, writing (review and editing). Stephen Bansberg: conceptualization, methodology, validation, supervision, writing (review and editing). Michael Marino: conceptualization, methodology, supervision, project administration, validation, writing (review and editing). All authors read and approved the final manuscript.

References

1. Ahn JC, Kim JW, Lee CH, Rhee CS (2016) Prevalence and risk factors of chronic rhinosinusitis, allergic rhinitis, and nasal septal deformity: results of the Korean National Health and Nutrition

Survey 2008–2012. JAMA Otolaryngol Head Neck Surg 142:162–167. https://doi.org/10.1001/jamaoto.2015.3142

2. Albert AM, Ricanek K Jr, Patterson E (2007) A review of the literature on the aging adult skull and face: implications for forensic science research and applications. Forensic Sci Int 172:1–9. https://doi.org/10.1016/j.forsciint.2007.03.015
3. Bastir M, Megía I, Torres-Tamayo N et al (2020) Three-dimensional analysis of sexual dimorphism in the soft tissue morphology of the upper airways in a human population. Am J Phys Anthropol 171:65–75. https://doi.org/10.1002/ajpa.23944
4. Cherobin GB, Voegels RL, Gebrim EMMS, Garcia GJM (2018) Sensitivity of nasal airflow variables computed via computational fluid dynamics to the computed tomography segmentation threshold. PLoS ONE 13:e0207178. https://doi.org/10.1371/journal.pone.0207178
5. Darbari Kaul R, Zhong W, Liu S et al (2025) Development of an open-source algorithm for automated segmentation in clinician-led paranasal sinus radiologic research. Laryngoscope 135:4125–4133
6. Daultrey C, Hardman J, Anari S (2018) The Caucasian nasal septum: an in vivo computed tomography study. Aesthet Surg J 38:717–722. https://doi.org/10.1093/asj/sjx248
7. Edelstein DR (1996) Aging of the normal nose in adults. Laryngoscope 106(9 Pt 2):1–25. https://doi.org/10.1097/00005537-199609001-00001
8. Fedorov A, Beichel R, Kalpathy-Cramer J et al (2012) 3D Slicer as an image computing platform for the Quantitative Imaging Network. Magn Reson Imaging 30:1323–1341. https://doi.org/10.1016/j.mri.2012.05.001
9. Godley FA (1997) Nasal septal anatomy and its importance in septal reconstruction. Ear Nose Throat J 76:498–506
10. Isensee F, Jaeger PF, Kohl SAA, Petersen J, Maier-Hein KH (2021) nnU-Net: a self-configuring method for deep learning-based biomedical image segmentation. Nat Methods 18:203–211. https://doi.org/10.1038/s41592-020-01008-z
11. Kazimierczak N, Kazimierczak W, Serafın Z et al (2023) Correlation analysis of nasal septum deviation and results of AI-driven automated 3D cephalometric analysis. J Clin Med 12:6621. https://doi.org/10.3390/jcm12206621
12. Kim SK, Na Y, Kim JI, Chung SK (2013) Patient specific CFD models of nasal airflow: overview of methods and challenges. J Biomech 46:299–306. https://doi.org/10.1016/j.jbiomech.2012.11.022
13. Li X, Morgan PS, Ashburner J, Smith J, Rorden C (2016) The first step for neuroimaging data analysis: DICOM to NIfTI conversion. J Neurosci Methods 264:47–56. https://doi.org/10.1016/j.jneumeth.2016.03.001
14. Loftus PA, Wise SK, Nieto D, Panella N, Aiken A, DelGaudio JM (2016) Intranasal volume increases with age: computed tomography volumetric analysis in adults. Laryngoscope 126:2212–2215. https://doi.org/10.1002/lary.25961
15. Mladina R, Skitarelić N, Poje G, Šubarić M (2015) Clinical implications of nasal septal deformities. Balkan Med J 32:137–146. https://doi.org/10.5152/balkanmedj.2015.159957

16. Noblitt B, Higgins J, Kopytek K, Brehm C, Gupta N (2023) The effect of segmentation threshold on computational fluid dynamic analysis of nasal airflow. J Craniofac Surg 34:337–342
17. Pessa JE, Zadoo VP, Mutimer KL et al (1998) Relative maxillary retrusion as a natural consequence of aging: combining skeletal and soft-tissue changes into an integrated model of midfacial aging. Plast Reconstr Surg 102:205–212
18. Russel SM, Frank-Ito DO (2023) Gender differences in nasal anatomy and function among Caucasians. Facial Plast Surg Aesthet Med 25:145–152
19. Sahu M, Xiao Y, Porras JL et al (2024) A label-efficient framework for automated sinonasal CT segmentation in image-guided surgery. Otolaryngol Head Neck Surg 171:1217–1225
20. Sramek M, Gibbs H, Casaday I et al (2026) Sexual dimorphism of the human nasal septum is a matter of size, not shape: three-dimensional morphometry of 1,373 adults. Submitted
21. Taha AA, Hanbury A (2015) Metrics for evaluating 3D medical image segmentation: analysis, selection, and tool. BMC Med Imaging 15:29. https://doi.org/10.1186/s12880-015-0068-x
22. von Elm E, Altman DG, Egger M, Pocock SJ, Gøtzsche PC, Vandenbroucke JP (2007) The Strengthening the Reporting of Observational Studies in Epidemiology (STROBE) statement: guidelines for reporting observational studies. Lancet 370:1453–1457. https://doi.org/10.1016/S0140-6736(07)61602-X
23. Wee JH, Kim DW, Lee JE et al (2012) Classification and prevalence of nasal septal deformity in Koreans according to two classification systems. Acta Otolaryngol 132(suppl 1):S52–S57
24. Whangbo J, Lee J, Kim YJ, Kim ST, Lee KS (2024) Deep learning-based multi-class segmentation of the paranasal sinuses of sinusitis patients based on computed tomographic images. Sens (Basel) 241933. https://doi.org/10.3390/s24061933
25. Wu Q, Xue N, Wang P et al (2022) Morphometric analysis of the nasal septum in normal Chinese individuals using a three-dimensional model of the nasal septum with facial CT scanning. Am J Transl Res 14:2609–2616
26. Zhai Q, Cui M, Fu Y et al (2025) Automated assessment of nasal septum deviation using cone-beam computed tomography images based on artificial intelligence: development and multicenter validation. Am J Orthod Dentofacial Orthop.
27. Zhang Y, Wang J, Pan T et al (2024) NasalSeg: a dataset for automatic segmentation of nasal cavity and paranasal sinuses from 3D CT images. Sci Data 11:1329. https://doi.org/10.1038/s41597-024-04166-w

Figures

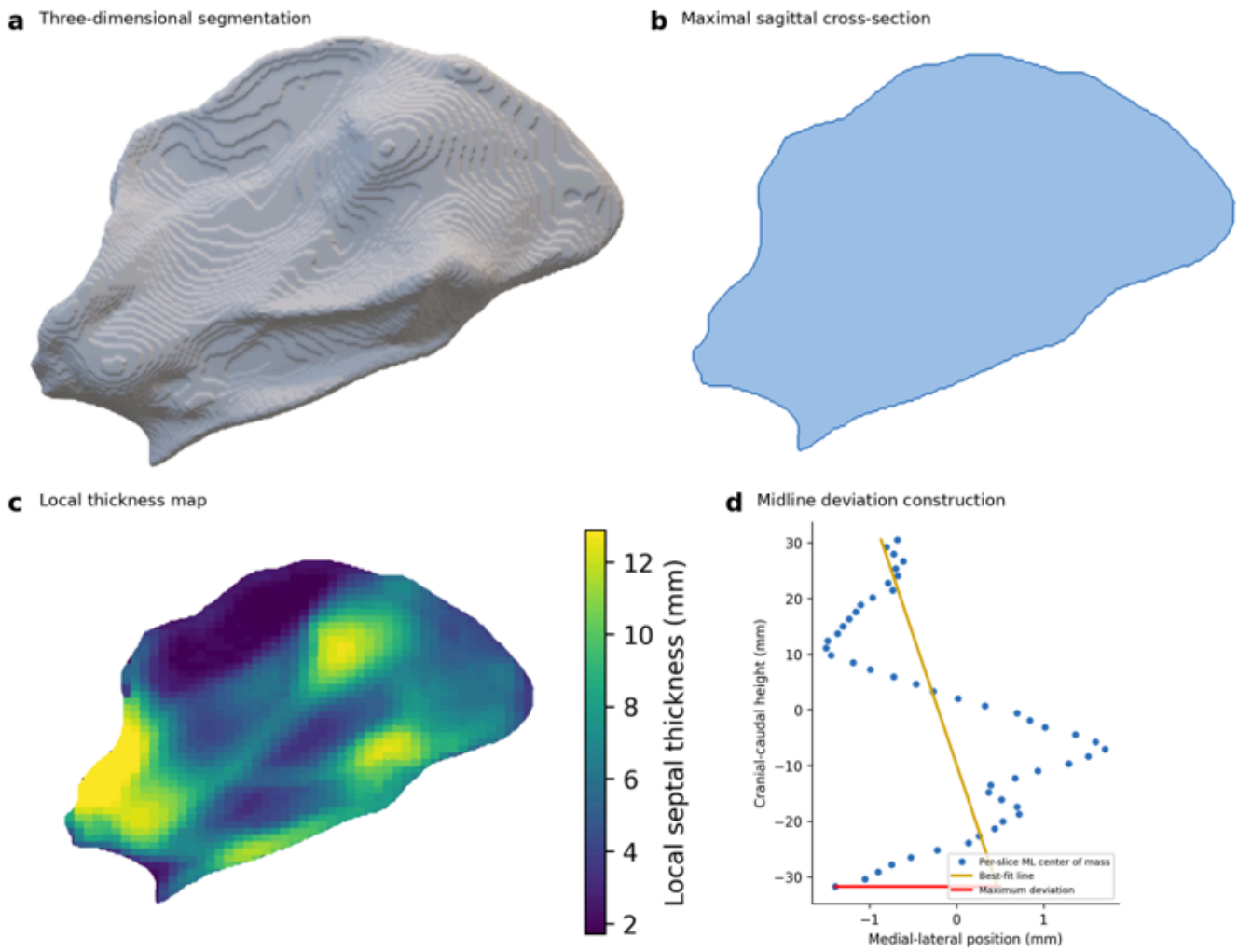


Figure 1

Segmentation-derived septal morphometric parameters, illustrated on one septum. **a**Three-dimensional surface rendering of an automated segmentation spanning the quadrangular cartilage, vomer, and perpendicular plate of the ethmoid, from the nasal floor to the skull base. **b** The parasagittal slice of maximal cross-sectional area. **c** Local thickness map, computed as twice the distance from each surface point to the medial skeleton of the septum; mean, 95th-percentile, and maximal thickness are summaries of this map. **d**Midline deviation construction: the medial-lateral centroid of the septum at each cranial-caudal level (points), the least-squares best-fit line (gold), and the maximal perpendicular distance of a centroid from the line (red), reported as the maximal midline deviation; the angle between the line and the cranial-caudal axis is the deviation angle

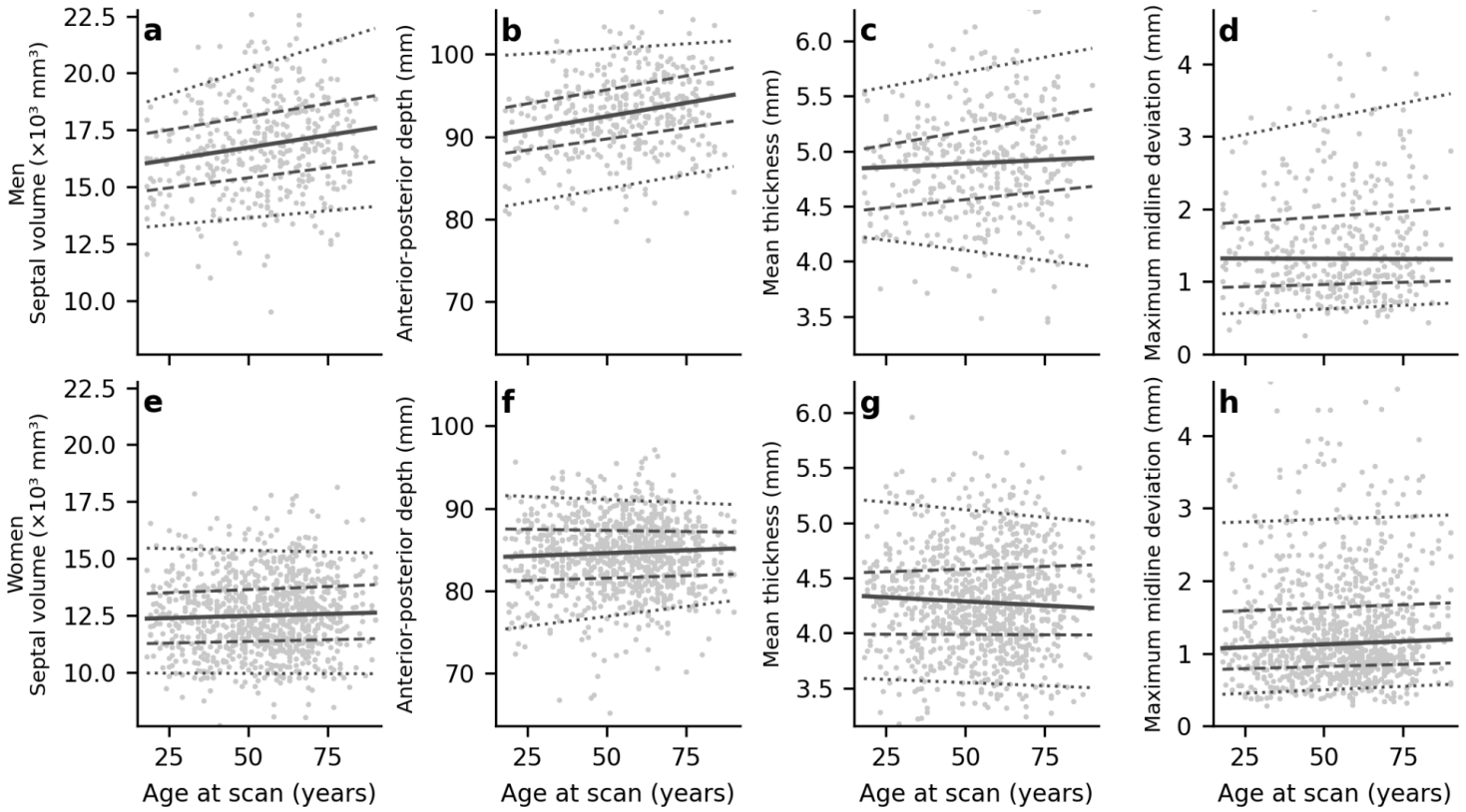


Figure 2

Age-specific reference centiles by sex for four parameters, from linear quantile regression on age: **a** to **d** men (n = 394), **e** to **h** women (n = 979). Solid line, median; dashed lines, 25th and 75th percentiles; dotted lines, 5th and 95th percentiles; points, individual values. Columns show septal volume, anterior-posterior depth, mean thickness, and maximal midline deviation. In men, volume and depth increase with age across the whole distribution; in women they are flat